CHEMICAL ENGINEERING TRANSACTIONS
VOL. 41, 2014
A publication of AIDIC
The Italian Association of Chemical Engineering
www.aidic.it/cet
Guest Editors: Simonetta Palmas, Michele Mascia, Annalisa Vacca

ISBN 978-88-95608-32-7; **ISSN** 2283-9216
DOI: 10.3303/CET1441066

MoS2 Nanosheets for HER and LIB

Maria Sarno, Anna Garamella, Claudia Cirillo*, Paolo Ciambelli

Department of Industrial Engineering and Centre NANO_MATES, University of Salerno
Via Giovanni Paolo II ,132 - 84084 Fisciano (SA), Italy
clcirillo@unisa.it

Very high surface area thin nanosheets of MoS_2, with also low lateral dimension, as well as high number of edges sites, were prepared via a solvent free, easily controllable and scalable process. The syntheses were performed by thermolysis of ammonium thiomolybdates $(NH_4)_2MoS_4$ in a continuous flow reactor, monitored with a mass spectrometer. The precursor decomposition was promoted in the temperature range 25-400°C, obtaining amorphous MoS2. Nanosheets were obtained thought a successive annealing, while material order can be improved by progressively increasing temperature and time. It was found that the annealing time at the end of the first step determines a reduction of the final nanosheets lateral size and number of layers. The samples were characterized by Raman Spectroscopy, Scanning (SEM) and Transmission (TEM-EDS) Electron Microscopy, thermogravimetric analysis (TG-DTG-MS), X-ray diffraction (XRD).

1. Introduction

MoS_2 nanostructure have generated intense scientific interest owing to their promising electronic and mechanical properties (Ramakrishna Matte et al., 2010), in the area of energy conversion and storage.
MoS_2 has been widely investigated as catalysts for electrocatalytic or photocatalytic hydrogen evolution reaction (HER) in aqueous solution and as efficient electrode material for lithium ion batteries (LIBs) (Zhao et al., 2013; Stephenson et al., 2014). Even if bulk MoS_2 is not active for the HER, it has been forecasted by using density functional theory calculation (Hinnemann et al., 2005) an excellent electrocatalytic activity (tafel slope 55–60 $mVdec^{-1}$), linearly dependent by the number of edge sites, for MoS_2 nanocatalyst (Jaramillo et al., 2007) prepared on an Au substrate. The same authors (Bonde et al., 2008) prepared later a more commercially relevant nanocatalyst, MoS_2 nanoparticles on a Toray carbon paper, finding higher tafel slope (120 mV/dec) and exchange current density. Further information about the electrocatalytic activity of MoS_2 comes form the paper of Merki et al. (Merki et al., 2011). They prepared amorphous thin films of MoS_x (about 1-2 μm thick), finding that the real catalyst was amorphous MoS_2, that exhibits a Tafel slope of 40 $mVdec^{-1}$. More recently, engineering the MoS2 structure, to have an high surface area mesostructure, exposing a large fraction of edge sites, a tafel slope of 50 mV/dec, has been found (Kibsgaard et al., 2012).
The reported results clearly demonstrate that the catalytic activity of MoS_2 toward the HER is very promising and closely associated with the different morphology of the prepared nanostructures. It deserves to be further investigated to definitely elucidate the effect of the support through a systematic comparison of the same nanostructured MoS_2 on a support and alone, and clarified the effect of order of the nanostructured materials prepared through a simple and scalable process.
MoS_2 is a conductive material characterized by a distinctive layered structure that makes it favorable for reversible Li+ intercalation/deintercalation (Xiao et al. 2010). The electrochemical performance of MoS_2 as a LIB electrode was believed to be significantly influenced by morphology, structure and particle size. The Li diffusion path could be significantly shortened in nanostructured MoS_2 improving the performance. As a nanostructure materials MoS_2 can exist in a diverse range of morphologies and microstructures. These include fullerene like MoS_2, MoS_2 nanotubes, MoS_2 nanowires, nanoribbons and nanosheets. In particular, with regards to this specific application, hydrothermal synthesized MoS_2 nanoflakes (Feng et al., 2009) and amorphous MoS_2 nanoflowers (Li et al., 2009) (prepared by an hydrothermal method), and nanotubes (Dominko et al., 2002) (prepared by a mixture of C60, used as promoter, and MoS_2 powder at 1010 K and

Please cite this article as: Sarno M., Garamella A., Cirillo C., Ciambelli P., 2014, Mos2 nanosheets for her and lib, Chemical Engineering Transactions, 41, 391-396 DOI: 10.3303/CET1441066

10^{-3} Pa), have been studied as anode materials and have been proven to have high capacity. On the other hand, at this stage the majority of the structures have not been investigated as electrode materials for lithium storage, the effect of the material order has not been clarified.

MoS_2 nanotubes (Loh et al., 2006), MoS_2 nanorods (Ota and Srivastava, 2006), MoS_2 nanofibers (Liao et al., 2001) and MoS_2 nanoflakes (Pol et al., 2008), have been synthesized. Moreover, after the discovery and the consequent enormous attention toward graphene properties and potential application, a growing research space is currently addressed to other 2-D materials and, among them, to layered inorganic materials such as dichalcogenides and especially MoS_2. In particular, for these specific applications the preparation of thin nanosheets, with also low lateral dimension, allows to have an high total surface area exposed, as well as a number of edges sites and short path for Li diffusion. Significant effort has been devoted to prepare MoS_2 thin layers. Several methods have been used to synthesize thin layers of MoS_2: scotch tape assisted micromechanical exfoliation, exfoliation in solution, physical vapor deposition, hydrothermal synthesis, electrochemical synthesis and sulfurization of oxides of molybdenum. However, the MoS_2 so produced tends to form structures similar to fullerene, zero-dimensional nanoparticles or nanotubes. A very interesting approach consists in a thermolysis of MoS_2 precursors in organic solvent (Altavilla et al., 2011). However, the products are often amorphous or low-crystalline and shown significant deficiency of molybdenum and the presence of impurities, such as carbon and oxygen.

Another method for producing thin layers of MoS_2 from amorphous to highly crystalline, with large surface area, consists of a solvent free thermolysis process (Liu et al., 2012). The method is one of the most scalable, permitting also, for example in presence of a template structure (Sarno et al., 2013; Ciambelli et al., 2011; Sarno et al. 2012), to prepare very promising carbon/MoS_2 composites (Zhao et al., 2013; Stephenson et al., 2014; Li et al. 2011).

Here we report, the synthesis of MoS_2 nanosheets, via a solvent free easily controllable and scalable process. MoS_2 nanosheets have been obtained by thermolysis of ammonium thiomolybdates $(NH_4)_2MoS_4$ in a continuous flow microreactor fed by nitrogen. The precursor decomposition was promoted in the temperature range 25-400°C, which permits to obtain amorphous MoS_2 sheets, followed by a second step in the range 25-1100°C to increasingly improve the starting material quality. In particular, the synthesis process was monitored with a mass spectrometer to follow the evolution of the reactions. Moreover, we have given much attention to the effect of changing the operating conditions, such as temperature, time and number of reaction steps, in view of a process/materials optimization. All the samples obtained were characterized by the combined use of different techniques such as micro-Raman Spectroscopy, Scanning Electron Microscopy (SEM), Transmission Electron Microscopy – Energy dispersive X-ray spectroscopy (TEM-EDS), thermogravimetric analysis coupled with a mass spectrometer (TG-DTG-MS), X-ray diffraction (XRD).

2. Experimental

MoS_2 nanosheets has been prepared by thermolysis of ammonium thiomolybdates $(NH_4)_2MoS_4$ (Sigma Aldrich, purity of 99.99%; 0.25g) in a N_2 environment, thought two steps of conversion: (i) from room temperature to 400°C + isotherm for 10 min (MoS2_1) or 60 min (MoS2_2); followed by (ii) a cooling from 400°C to room temperature; and finally (iii) a step from room temperature to 1100°C + isotherm for 30 min (MoS2_3 from MoS2_1 and MoS2_4 from MoS2_2) or 75 min (MoS2_5 from MoS2_2).

The annealing was carried out in a continuous flow microreactor, consisting in a quartz tube (16 mm internal diameter, 300 mm length), the precursor was loaded on a sintered support (Ciambelli et al., 2011; Sarno et al., 2013). All the samples obtained were characterized by the combined use of different techniques. Transmission electron microscopy (TEM) images were acquired using a FEI Tecnai electron microscope operated at 200 KV with a LaB6 filament as the source of electrons, equipped with an EDX probe. Scanning electron microscopy (SEM) images were obtained with a LEO 1525 microscope. Raman spectra were obtained at room temperature with a micro-Raman spectrometer Renishaw inVia with a 514 nm excitation wavelength (laser power 30 mW) in the range 100-3000 cm^{-1}. Optical images were collected with a Leica DMLM optical microscope connected on-line with the Raman instrument. For all the sample about 40 measurements have been carried out. The laser spot diameter was about 10 μm. XRD measurements were performed with a Bruker D8 X-ray diffractometer using CuK_α radiation. Thermogravimetric analysis (TG-DTG) at a 10 K/min heating rate in flowing air was performed with a SDTQ 500 Analyzer (TA Instruments) coupled with a mass spectrometer.

3. Results and discussion

The thermolysis of ammonium thiomolybdates $(NH_4)_2MoS_4$ has been extensively studied (Berntsen et al., 2008; Brito et al., 1995; Leist et al., 1998). It has been reported that $(NH_4)_2MoS_4$ thermolysis in an N_2 environment resulted in the conversion of $(NH_4)_2MoS_4$ to MoS_3, releasing ammonia and hydrogen sulfide to the gas phase ($(NH_4)_2MoS_4 \rightarrow 2NH_3 + H_2S + MoS_3$) at lower temperatures, followed by a conversion of MoS_3 to highly disordered MoS_2 (MoS3 → MoS2 + S), the product remained amorphous up to around 350°C, while crystallinity set in at 400°C when first vague lines appeared on the diffractograph. To improve the MoS_2 quality, it is rational to increase the thermolysis temperature. Although a measure of agreement is evident in the previous studies, there is ambiguity in the transition temperatures, nor systematic nanostructures synthesis studies have been performed. We develop the syntheses in two steps, the first one between 25-400°C, to obtain disordered MoS_2, further annealed for 10 or 60 min, the second step between 25 to 1100°C, followed by 30 or 75 min of annealing to further improve the degree of order. We prepared two different kinds of materials: low crystallinity samples at 400°C and high crystallinity samples at 1100°C, and following the evolution of the precursor thermolysis with the help of a thermogravimetric analyser. In particular, in Figure 1a the thermogravimetric (TG-DTG) and temperature profiles, during the test simulating the MoS2_5 synthesis conditions, characterized by the two longer isotherm steps, are reported as function of time. It is possible to distinguish five temporal phases: (I) from room temperature to 400°C; (II) 1h in isotherm at 400°C; (III) from 400°C to room temperature (not followed by the thermobalance); (IV) from room temperature to 1100°C; (V) 630 min in isotherm at 1100°C. After an initial weight loss due to water, at temperatures between 150-250°C the DTG profile shows a sharp weight loss due to NH_3 and H_2S release, as clearly indicated by the corresponding total ion current (TIC) of the most intense mass fragments peaks: m/z = 15, 16, 17 form NH3 and 32, 33, 34 from H2S (reaction 1). The NH_3 and H2S release completing at 360°C. At 170°C a sulphur release starts, with a maximum at 380°C, compatible with the evolution of reaction 2. A further 3 wt.% is lost in the 60 min isothermal step at 400°C. During the further temperature increase (phase IV) and starting from 400°C a sulphur release (m/z=32) happens. A weight loss is also registered during the high temperature isotherm, due to an intrinsic MoS_2 thermal instability (Spalvins, 1987) and the unavoidably few trace of oxygen, with SO2 (m/z=64) release and contemporaneous formation of oxides.To follow the crystallization, XRD patterns were recorded on the decomposition products after heating at specific temperatures (Figure 1b). Both MoS2_1 and MoS2_2 exhibit the loss of the original precursor structure and the typical x-ray pattern of amorphous MoS_2, the (002) reflection results broader and less intense if compared with the rest of the spectrum for sample annealed for 60 min, indicating an exfoliation tendency for longer time annealing. After the second step of thermolysis the typical spectrum of 2H-MoS_2 is shown for both MoS2_3 and MoS2_4, a very broad (002) reflection is shown in the spectrum of MoS2_4 (Berntsen et al., 2008; Leist et al., 1998), while MoS2_3 exhibits a more pronounced sawtooth (002) peak, sharper and less intense if compared with MoS2_1. At increasing high temperature annealing time, the peak at about 13° (2Θ) becomes more and more pronounced and sharper, indicating a progressive in-plane restacking, also the typical MoO_2 peaks appear timidly, likely due to an initial oxidation phenomenon. Similar to the case of graphene, Raman spectroscopy can be employed to characterize the thickness of MoS_2 nanolayers (Castellano-Gomez et al., 2012; Lee et al., 2010). The bulk MoS_2 shows bands at 407.5 and 382 cm^{-1} due to the A_{1g} and E'_{2g} modes (Li et al., 2012). As reported by Lee et al. (Lee et al., 2010), the frequency difference between the two most prominent Raman peaks depends monotonically on the number of MoS_2 layers. In particular, in Figure 2 number of significant Raman spectra are reported for MoS2_4, MoS2_3 and MoS2_5, most of MoS2_4 and MoS2_3 sheets have lower than 6 layers, while MoS2_5 sheets are decidedly thicker, in agreement with the XRD observation. It is worth to notice the presence in MoS2_3 of sheets consisting of more than 10 layers if compared with MoS2_4.

For comparison, MoS2_1, MoS2_3 and MoS2_4 micrographs are shown in Figure 3, it is evident in the resolution limits of the instrument, a delamination of the MoS2_1 powders after the second step of thermal treatment (compare Figures 3d and 3e). Finally, MoS2_4 consists of lower size powders with a rougher surface. Figure 3g shows the complete N_2 adsorption-desorption isotherm of MoS2_3, it presented a well-developed porous structure with a type IV isotherm, which had an obvious hysteretic loop with a desorption step above the relative pressure of 0.4.

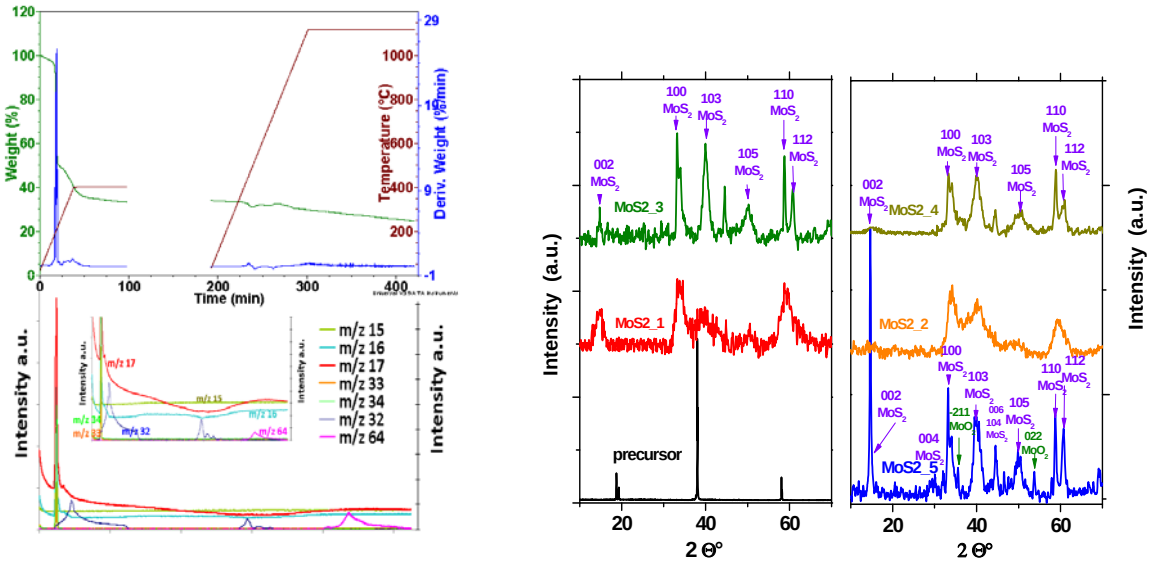

Figure 1. TG-DTG profiles, during the test simulating the MoS2_5 synthesis conditions, and the corresponding TIC (a). XRD diffraction patterns of the precursor and samples after heating at the different temperatures (b).

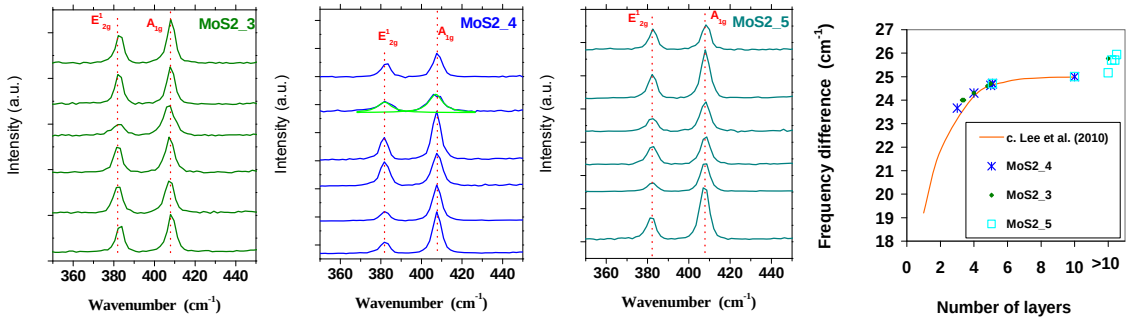

Figure 2. Raman Spectra of MoS2_3, MoS2_4, MoS2_5 and the frequency difference between A_{1g} and E'_{2g} Raman modes

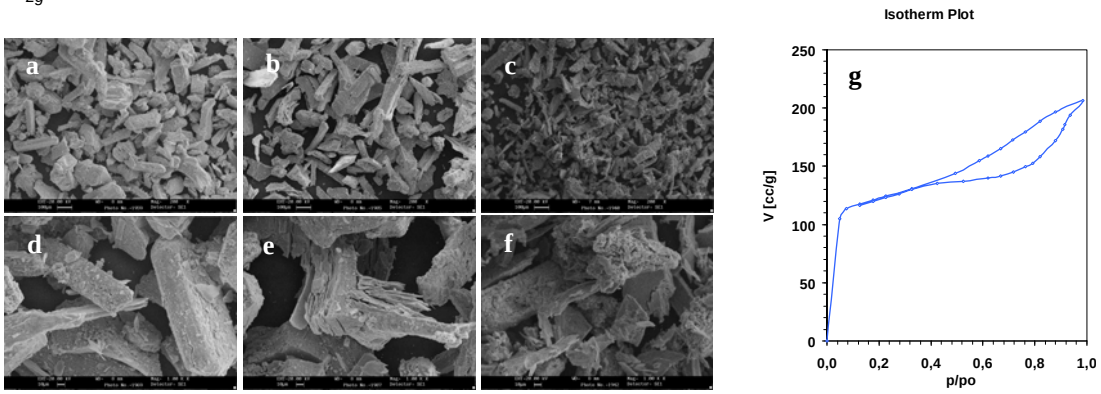

Figure 3 SEM images of MoS2_1 (a), MoS2_3 (b) and MoS2_4 (c) - 200X, scale bar 100 μm. SEM images of MoS2_1 (d), MoS2_3 (e) and MoS2_4 (f) - 1000X, scale bar 10 μm. N_2 adsorption-desorption isotherm of MoS2_3 (g).

The MoS2_3 BET surface areas (SA) is 208 m^2/g, a very high value if compared with that reported for conventional MoS_2 prepared by thermal decomposition of MoS_2 precursors (from 49.3 to 64.4 m^2/g in Leist et al. (Leist et al.,1998), where the authors speculated that both the heat treatment and the presence of vacuum are necessary for porous material to be obtained and compared their results with the BET surface

areas of crystalline 5.8 m^2/g and restacked 10 m^2/g MoS_2). BET SA of 40 m^2/g and 77.7 m^2/g has been reported for conventional MoS_2 in (Skrabalak et al., 2005) and (Berntsen et al., 2003), respectively. A solvothermal route was explored in (Berntsen et al., 2003) to obtain a BET of 152.9 m^2/g and an ultrasonic spray pyrolysis in (Skrabalak et al., 2005) to obtain a surface area of 250 m^2/g. MoS2_3 has a total pore volume of 300.01 mm^3/g, and a multimodal pore size distribution (BJH Desorption pore distribution) centred at 2, 3, 7, 10 and 15 nm (pores between exposed surface sheets). It is worth to notice that the BET SA of MoS2_1 is 2.88 m^2/g, while the MoS2_4 SA results 260 m^2/g.

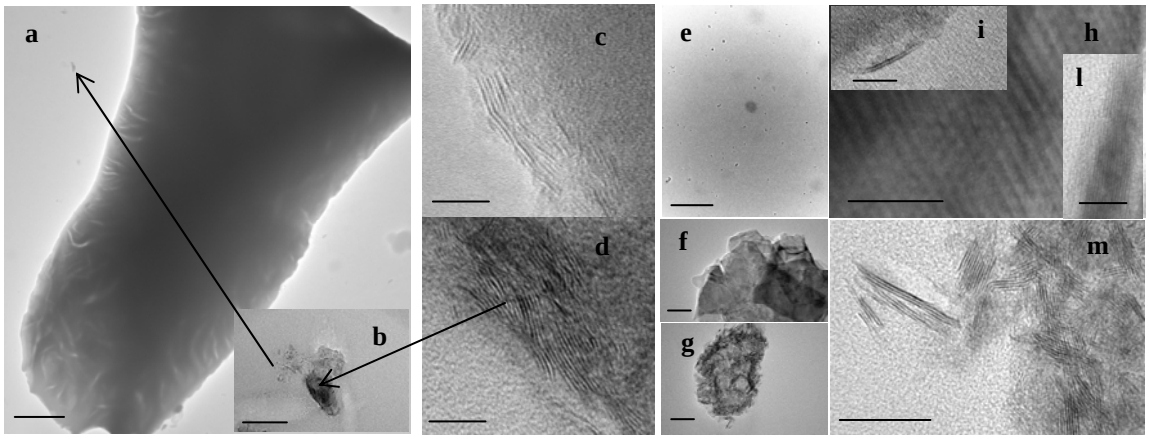

Figure 4 TEM images of MoS2_1 scale bar 2μm (a), scale bar 500 nm (b), scale bar 10 nm (c,d). TEM images of MoS2_2 scale bar 1μm (e). TEM images of MoS2_3 scale bar 50 nm (f), scale bar 20 nm (h), scale bar 10 nm (i.l). TEM images of MoS2_4 scale bar 50nm (g), scale bar 20 nm (m).

Typical TEM image of the MoS2 samples are shown in Figure 4. MoS2_1 (Figure 4a) is constituted of larger (tens of microns in size) and smaller few aggregates (1 micron in size); MoS_2 layers, 0.62 nm stacked, are visible in both aggregates (Figure 4c and d). The Figure 4e shows MoS2_2, constituted of small particles with size of few hundred nanomaters. MoS2_3 (Figure 4f) and MoS2_4 (Figure 4g), obtained at the end of the second step and after 30 min of annealing, exhibit a different morphology. MoS2_3 is constituted of larger sheets consisting of few layers or more than 10 layers (inserts of Figure 4h), moreover smaller sheets of few nanometers lateral size with the characteristic MoS2 fringes can be observed in the figures 4g and 4m for MoS2_4.

4. Conclusions

Very high surface area thin nanosheets of MoS2, with also low lateral dimension were prepared via a solvent free, easily controllable and scalable process. The precursor decomposition was promoted in the temperature range 25-400°C, obtaining amorphous MoS2. Nanosheets were obtained thought a successive annealing, while material order can be improved by progressively increasing temperature and time. It was found that the annealing time at the end of the first step determines a reduction of the final nanosheets lateral size and number of layers.

References

Altavilla C., Sarno M., Ciambelli P., 2011, A Novel Wet Chemistry Approach for the Synthesis of Hybrid 2D Free-Floating Single or Multilayer Nanosheets of MS2@oleylamine (MdMo, W), Chem. Mater. 23, 3879–3885;

Berntsen N., Gutjahr Tobias, Loeffler Lars, Gomm John R., Seshadri Ram, Wolfgang Tremel, 2008, A Solvothermal Route to High-Surface-Area Nanostructured MoS2, Chem. Mater 15, 4498-4502;

Bonde J., Moses P. G., Jaramillo T. F.,. Norskov J.K., Chorkendorff I., 2008, Hydrogen evolution on nano-particulate transition metal sulfides, Faraday Discuss. 140, 219-231.

Brito, J. L., Ilija, M., Hernfindez, P., 1995, Thermal and reductive decomposition of ammonium thiomolybdates, Thermochim. Acta., 256, 325-338.

Castellano-Gomez A., Barkelid M., Goossens A. M., Caldo V. E., van der Zant H. S. J., Steele G. A., 2012, Laser-Thinning of MoS2: on demand Generation of a single-layer semiconductor, Nanoletters 12, 3187-3192.

Ciambelli P., Arurault L., Sarno M., Fontorbes S., Leone C., Datas L., Sannino D., Lenormand P., Le Blond Du Plouy S., 2011, Controlled growth of CNT in mesoporous AAO through optimized conditions for membrane preparation and CVD operation, Nanotechnology 22, 265613.

Dominko R., Arcon D., Mrzel A., Zorko A., Cevc P., Venturini P., Gaberscek M., Remskar M. Mihailovic D., 2002, Dichalcogenide Nanotubes Electrode for Li-ion Batteries, Adv. Mater. 14, 1531-1534.

Feng C., Ma J., Li H., Zeng R., Guo Z., Liu H., 2009, Synthesis of molybdenum disulfide (MoS2) for lithium ion battery applications, Mater. Res. Bull. 44, 1811-1815.

Hinnemann B., Moses P. Georg, Bonde J., Jørgensen K.P., Horch J. H. Nielsen S., Chorkendorff I., Nørskov J. K., 2005, Biomimetic Hydrogen Evolution: MoS_2 Nanoparticles as Catalyst for Hydrogen Evolution, J. Am. Chem. Soc. 127, 5308-5309.

Jaramillo T.F., Jørgensen K. P., Bonde J., Nielsen J. H., Horch S., Chorkendorff I., 2007, Identification of Active Edge Sites for Electrochemical H_2 Evolution from MoS_2 Nanocatalysts, *Science* 317, 100-102.

Kibsgaard J., Chen Z., Reneicke B. N., Jaramillo T.F., 2012, Engineering the surface structure of MoS_2 to preferentially expose active edge sites for electrocatalysis, Nat. Mater. 11, 963-969.

Lee C., Yan H., Bruns L. E., Heinz T. F., Hone J., Ryu S., 2010, Anomalous lattice vibrations of single- and few-layer MoS2, ACS Nano 4, 2695-2700.

Leist A., Stauf S., Loken S., Finckh E.W., Ludtke S., Unger K. K., Assenmacher W., Maderb W., Tremela W., 1998, Semiporous MoS_2 obtained by the decomposition of thiomolybdate precursors, J. Mater. Chem. 8, 241-244.

Li H., Li W., Ma L., Chen W., Wang J., 2009, Electrochemical lithiation/delithiation performances of 3D flowerlike MoS_2 powders prepared by ionic liquid assisted hydrothermal route, J. Alloys Comp. 471, 442-447.

Li H., Q. Zhang, C. Chong, 2012, From bulk to monolayer MoS2: Evolution of Raman Scattering, Adv functional Materials 22, 1385-1390.

Li Y., Wang H., Xie L., Liang Y., Hong G., Dai H., 2011, MoS_2 Nanoparticles Grown on Graphene: An Advanced Catalyst for the Hydrogen Evolution Reaction, J. Am. Chem. Soc. 133, 7296–7299.

Liao H. W., Wang Y. F., Zhang S. Y., Qian Y. T., 2001, A Solution Low-Temperature Route to MoS2 Fiber, Chem. Mater. 13, 6-8.

Liu K.K., Zhang W., Lee Y.H., Lin Y.C., Chang M.T., Su C.Y., Chang C.S., Li H., Shi Y., Zhang H., Lai C.S., Li L.J., 2012, Growth of Large-Area and highly crystalline MoS_2 thin layers on insulating substrate, Nano Letters 12, 1538-1544.

Loh K. P., Zhang H., Chen W. Z., Ji W., 2006, Templated Deposition of MoS_2 Nanotubules Using Single Source Precursor and Studies of Their Optical Limiting Properties, J. Phys. Chem. B 110,1235-1239.

Merki D., Fierro S., Vrubel H., Hu X., 2011, Amorphous molybdenum sulfide films as catalysts for electrochemical hydrogen production in water, Chem. Sci. 2, 1262-1267.

Ota J.R. and Srivastava S.K., 2006, A new Hydrothermal route for synthesis of molybdenum disulphide nanorods and related nanostructures, J. Nanosci. Nanotechnol. 6, 168-174.

Pol V.G., Pol S.V., George P.P., Gedanken A., 2008, Combining MoS_2 or $MoSe_2$ nanoflakes with carbon by reacting $Mo(CO)_6$ with S or Se under their autogenic pressure at elevated temperature, J. Mater. Sci. 43, 1966-1973.

Ramakrishna Matte H. S. S., Gomathi A., Manna A. K., Late D. J., Datta R., Pati S. K., Rao C. N. R., 2010, MoS_2 and WS_2 Analogues of Graphene, Angew. Chem.122, 4153-4156.

Sarno M., Tamburrano A., Arurault L., Fontorbes S., Pantani R., Datas L., Ciambelli P., Sarto M.S., 2013. Electrical conductivity of carbon nanotubes grown inside a mesoporous anodic aluminium oxide membrane, Carbon 55, 10-22.

Sarno M., Sannino D., Leone C., Ciambelli P., 2012, Evaluating the effects of operating conditions on the quantity, quality and catalyzed growth mechanisms of CNTs, J. Mol. Catal. A: Chem. 357, 26-38.

Skrabalak S.E., Suslick K.S., 2005, Porous MoS_2 synthesized by ultrasonic spray pyrolysis, J. Am. Chem. Soc. 127, 9990-9991.

Spalvins, T., 1987, A review of recent advances in solid film lubrication, J. *Vac. Sci. Technol*. A 5, 212-219.

Stephenson T., Li Z., Plsen B., Mittlin D., 2014, Lithium ion battery applications of molybdenum disulfide (MoS2) nanocomposites, Energy and Environ. Sci. 7, 209-231.

Xiao J., Choi D., Cosimbescu L., Koech P., Liu J., Lemmon J. P., 2010, Exfoliated MoS_2 Nanocomposite as an Anode Material for Lithium Ion Batteries, Chem. Mater. 22, 4522-4524.

Zhao Y., Zhang Y., Yang Z., Yan Y., Sun K., 2013, Synthesis of MoS_2 and MoO_2 for their applications in H_2 generation and lithium ion batteries: a review, Sci. Technol. Adv. Mater. 14, 043501 (12pp).